J. Eng. High. Tech., 1(1)1-8,2015

ISSN 2356-8860
Journal of Engineering and Higher Technology (JEHT)
www.textroad.com

Poly (methyl methacrylate)/Single Walled Carbon Nanotube (PMMA/SWCNT) Nanocomposites: Optical and Electrical Characterization

F.S. Thabet[a], F. Yakuphanoglu[b], G.M. Nasr[c], Sh.A. Mansour[d]

[a] Physics Department, Faculty of Science, Taiz University, Yemen
[b]Physics Department, Faculty of Science, Firat University,23119, Elazig, Turkey
[c]Physics Department, Faculty of Science ,Cairo University, Egypt
[d]Department of Basic Engineering Science, Faculty of Engineering, Menofia University, Egypt

Received: January 27, 2015
Accepted: March 31, 2015

ABSTRACT

The effects of single walled carbon nanotube (SWCNT) on the optical and electrical properties of polymethyl methacrylate have been investigated. Optical parameters such as absorption, direct band gap, and indirect band gap were determined for PMMA/SWCNT composites from their optical reflectance spectra in the wavelength range 200-900 nm. It is found that the energy gap and band edge values are shifted to lower energies with increase of the SWCNT content. The electrical conductivity was measured as a function of temperature from 298K to 373K. The electrical conductivity of the nanocomposites increases with increasing the temperature. The charge transport mechanism is controlled by variable range hopping conduction mechanism for PMMA/SWCNT nanocomposites.
KEYWORDS: Nanocomposites, Carbon nanotubes, Semiconductor

INTRODUCTION

The electrical and optical properties of insulating polymers can be changed by the presence of nanoparticles such as carbon nanotubes. The carbon nanotubes (CNTs) have been extensively investigated to produce new advanced composite materials [1]. Ajayan et al. firstly have incorporated CNT in an epoxy matrix [2], till now, CNT have been used as fillers in the insulating polymer matrices to improve the mechanical and electrical properties [2,3]. Amongst the insulating polymers, poly (methyl methacrylate) (PMMA) has received a great interest due to its interesting optical and electrical properties. This polymer is the thermoplastic material and it has a good tensile strength and hardness, high rigidity, transparency, good insulation properties [4-6]. PMMA/CNT composites can be used for the application as electromagnetic interference (EMI shielding materials [7], transparent conducting films [8-9], gas sensors [10, 11], etc. In present study, our aim is to characterize the optical and electrical properties through the transformation of the insulating such as PMMA polymer to semiconducting one by addition of single wall carbon nanotube (SWCNT). For this, we synthesized PMMA using free radical polymerization method and prepared PMMA/ SNCNT nanocomposites with different weight percentage of SWCNT from 1% to 16%.

2. EXPERIMENTAL DETAILS

2.1 Preparation of the Composites

Methyl methacrylate (MMA) (Fluka), azobisisobutyronitrile (AIBN) (Fluka), dimethyl formamide (DMF) (Aldrich), single wall carbon nanotubes (SWCNT) (Aldrich) and other chemicals and solvents were used without further purification. Polymerization of methyl methacrylate was performed by using free radical polymerization method. In this process, 0.08 wt.% of free radical initiator-AIBN (2,2%-azobisisobutyronitrile) is added into MMA at the reaction temperature at 70 ^{o}C. After synthesis of the poly (methyl methacrylate), the PMMA-single wall nano tube composites were produced by the coagulation method. For this purpose, 1 g of poly (methyl methacrylate) was dissolved 10 mL of DMF. Different weight ratios (1%, 4%, 8%, 12% and 16%) of SWCNT were dispersed in 2 mL of DMF for 10 hours using ultrasonic bath. After that, the polymeric solution was added to the dispersed SWCNT in DMF and stirred the mixture by using magnetic stirrer for 2 hours. The polymer-nanotubes composites were obtained by evaporating solvent under vacuum. The prepared nanocomposites were formed in the form of pellet by applying 10 ton.

*** Corresponding Author:** F.S. Thabet, Physics Department, Faculty of Science, Taiz University, Yemen.
E-mail:fairoz_sth2008@yahoo.com

2.2 Characterization of the composites

The UV–VIS spectra of the samples were recorded from 200 to 1000 nm wavelength using a SHIMADZU UV-3600 UV–VIS–NIR spectrophotometer at room temperature. The electrical conductivity measurements were performed with a KEITHLEY 6517A by alternating polarity method.

3. RESULTS AND DISCUSSIONS

3.1 Optical characterization of the synthesized PMMA/SWCNT nanocomposites

In order to study the optical properties of the synthesized *PMMA/SWCNT* nanocomposites pellets, the UV-vis diffuse reflectance spectrum was measured as shown in Fig. 1. Figure 1 reflects that, the average reflectance of the (PMMA/SWCNT) composites is decreased with increasing SWCNT content in the UV region. The optical band gap of the samples is determined from the absorption spectra near the absorption edges.[12]. For determination of the optical band gap of PMMA/SWCNT composites, we converted the reflectance values to absorbance values by means of by Kubelka–Munk function [13, 14]. In this function, the diffuse reflectance spectra are obtained from weakly absorbing samples. This function can be determined by the following relation [13, 14]:

$$F(R) = \frac{(1-R)^2}{2R} \qquad (1)$$

where R is the diffused reflectance. F(R) is Kubelka–Munk function. We converted F(R) values to the linear absorption coefficient by the following relation [14,15].

$$\alpha = \frac{\mathrm{F(R)}}{\mathrm{t}} = \frac{\mathrm{Absorbance}}{\mathrm{t}} \qquad (2)$$

where t is the thickness of samples. The relation between absorption and optical band gap for many materials can be expressed by [16-18]

$$\alpha h\upsilon = A\left(h\upsilon - E_g\right)^n \qquad (3)$$

where, , h is Planck's constant, ν is the frequency of the incident photons, , A is constant depending on the transition probability [16,19], E_g optical energy band gap, and n is a exponent which has discrete values like 1/2, 3/2, 2 or more depending on whether the transition is direct or indirect and allowed or forbidden, respectively. In the direct and allowed cases, the index n = 1/2 whereas for the direct but forbidden cases it is 3/2. But for the indirect and allowed cases n = 2 and for the forbidden cases it is 3 or more. One can rewrite Eq.3 as;

$$\left(\frac{\mathrm{F(R)h\upsilon}}{\mathrm{t}}\right) = \beta\left(h\upsilon - E_g\right)^n \qquad (4)$$

In this respect, Fig. 2 shows the plot between $\left(\frac{F(R)h\upsilon}{t}\right)^2$ and hν which shows a linear portions indicates that the transition through direct band gap. The obtained values of the optical energy band gaps (E_g) of the nanocomposites were determined from Fig.2 and are given in Table 2.

In order to clarify an extending band tails for lower photon energies below the band edge [20-22], we used the following relation,

$$\alpha = \alpha_0 \exp\left(\frac{E}{E_u}\right) \qquad (5)$$

where E_u is the energy of Urbach corresponding to the width of the band tails of localized states in the band gap. Fig.3 shows the plots of (ln α) versus hν for the samples. The values of E_u were calculated as the reciprocal gradient of the linear portion of Fig.3. The obtained Urbach energy E_u values for PMMA-SWCNT samples are given in Table 1. It is seen that the optical band gap of the samples is decreased from 4.05 for pure PMMA [23, 9, and 10] to 2.4 as SWCNT concentration increase up to 12%. This change is due to increasing the concentration of electron of SWCNT. The narrowing band gap energy is possibly due to the existence of SWCNT impurities in the PMMA structure, which induce the formation of new recombination centers with lower emission energy .The shift of absorption edge for samples including with 16%SWCNT may be due to an increase in carrier concentrations which lead to the Burstein–Moss effect [24]. The low value of E_u was obtained for high concentration of SWCNT (16%) in PMMA and can be attributed to the less effect of internal potential fluctuation associated with the structural order [20].

Also, the optical properties of the samples can be characterized by the complex refractive index. The complex refractive index is expressed as

$$n* = \mathrm{n(w)} + \mathrm{ik(w)} \qquad (6)$$

where *n* is the real part and *k* is the imaginary part. *n* can be obtained by using the following equation [5,25]

$$n = \frac{1+R}{1-R} + \sqrt{\frac{4R}{(1-R)^2} - k^2} \qquad (7)$$

where k=αλ/4π.is the extinction coefficient .The plots of refractive index for the samples are shown in Fig. 4. As seen in Fig. 4, the n values is increased with increasing SWCNT up to 4% with respect the n value of pure PMMA after that it is decreased with increasing SWCNT content. The refractive index of PMMA is normally about 1.49. The refractive index of the PMMA-SWCN composite in the visible region was found to be, 1.52, 1.54, 1.49, 1.5 and 1.45 for PMMA 1%, 4% , 8% , 12% and 16% SWCNT, respectively. The decrease in the refractive index may be due to the increase of SWCNT content. This is attributed to decrease in the polarizability, which is associated with carbon electron incorporation. At the same time, the variation of sample density causes the decrease in refractive index as well. The higher this density is, the higher the refractive index [25,26].

3.2 Electrical properties of the nanocomposites

The electrical conductivities of the nanocomposites were measured in the temperature range (298–373 K). For the analysis of electrical conductivity, we used Arrhenius relation given by [27]:

$$\sigma = \sigma_0 \exp\left(-\frac{E_a}{kT}\right) \qquad (8)$$

where σ_o is the pre-exponential factor, E_a is the activation energy of the electrical conduction, k is the Boltzmann constant and T is the absolute temperature. The activation energy for the samples was determined from the plots of ln (σ) vs. 1000/T (Fig5). These plots exhibit more than one straight line for most prepared samples associated with different conduction mechanism. The conductivity of the samples is increased with increasing temperature. This confirms that the samples exhibit the semiconducting behavior except 1% SWCNT doped PMMA. The activation energy values for the investigated samples are given in Table 2. As seen in Table 2, the activation energies are decreased with the SWCNT contents.

The most common conduction mechanism followed by polymer composites and other disordered semiconductor is variable range hopping (VRH) conduction. The Mott́s VRH formalism for phonons on small polarons for conductivity of disordered semiconductor materials [28, 29] will be described here in summary. Depending on the dimensionality of the system, i.e, and d = n-1, the temperature dependent VRH conductivity is given by:

$$\sigma = \sigma_0 \exp\left[-\left(\frac{T_0}{T}\right)^{1/n}\right] \qquad (9)$$

Where σ_0 is the high temperature limit of conductivity and T_0 the Mott́s characteristic temperature associated with the electronic wave function localization degree. The exponent n assumes 4, 3 and 2 for three-two and one-systems respectively. Mott temperature T_0 for three dimensional variable hopping conduction mechanism can be expressed by the following relation,

$$T_0 = \frac{\lambda}{k_B \eta(E_F)\, a^3} \qquad (10)$$

Where λ is dimensionless constant (≈18.1) [30, 31], k_B is the Boltzmann constant, **a** wave function localization radius, and $\eta(E_F)$ is the density of state at the Fermi level. If the density of states is not constant near the Fermi level and has quadratic dependence, equation (11) is determined by Efros-Shklovskii VRH with exponent n=2. From Figure (6), which represent the temperature dependence of conductivity for all samples. One could notice that the VRH is observed for the samples except for sample included 1%SWCNT. For sample including 16% SWCNT, the particles at relatively higher temperatures are affected by differential thermal expansion between carbon and polymer, which reduces the tunneling conduction and hopping conduction mechanism.

The conductivity as function of $T^{-1/2}$ and $T^{-1/4}$ is shown in Fig.7. The conductivity as a function of temperature (both for $T^{-1/2}$ and $T^{-1/4}$) at different temperature regions exhibits straight line behavior with regression factors as indicated in figures. The value of T_0 can be obtained from the experimental data through fittings to Eq.11, usually in a linearized form. From T_0 one can calculate η(EF), which is used to determine the mean hopping distance R [31], the mean density of hopping carriers N, and the mean energy necessary for a hop [32].

$$R = \left[\frac{9a}{(8\pi k_B\ T\eta(E_F))}\right]^{1/4} \qquad (11)$$

$$N = \frac{3}{4\pi R^3} \quad (12)$$

$$E = \frac{N}{\eta(E_F)} \quad (13)$$

Considering the conduction mechanism, since the best linear fitting to σ are obtained for these samples in Figures (7), we conclude that the (3D) and 1D-VRH charge transport occurs in samples doped with 4% and 8% SWCNT for different temperature regions, meanwhile the samples including 12% and16%SWCNT particle reveal (1D) VRH charge transport for all temperature region. T_0 analyze the data using Mott's variable range hopping theory, it is assumed that the localization length **a** is 1.5 A^0 as proposed by Ganpopadhyay et al (31). Table (3) presents the different parameters obtained by fitting the experimental results to the Mott's VRH theory. Combining equation (12) and (13) we conclude that larger T_0 implies larger R. Therefore, the conductivity decreases with T_0. Also high T_0 implies larger hopping distances, and larger energies for a hop. Comparing our results with those from the literature (Table 4), it can be seen that our samples have intermediate conductivities.

Table 1. Values of the band gap E_g and Urbach energy E_u for PMMA-SWCNT samples

Content of SWCNT	E_g (ev)	E_u (ev)
1%	4.05	0.2616
4%	3.2	0.32
8%	2.49	0.158
12%	2.4	0.266
16%	3.34	0.105

Table 2. Activation energy values for PMMA-SWCNT samples

Sample	E_a (eV) for region (I)	E_a (eV) for region (II)	E_a (eV) for region (III)
PMMA-4%SW CNT	0.5	0.26	0.05
PMMA-8%SW CNT	0.33	0.09	0.04
PMMA-12% SWCNT	0.25	0.19	0.01
PMMA-16% SWCNT	0.07	0.04	-------

Table (3) Present the different parameters obtained by fitting the experimental results to the Mott's VRH equations

Region(1)					
Content of SWCNT	T_0	$\eta(cm^{-3}/mev$	$Rx10^{-7}$ (cm)	N (cm^{-3})	E (mev)
4%	$4.23x10^{9}$	$1.47x10^{19}$	3.45	$5.81x10^{18}$	395
8%	$1.87x10^{5}$	$3.33x10^{23}$	.280	$1.08x10^{22}$	32
12%	$3.1x10^{4}$	$9.24x10^{25}$	0.068	$7.3x10^{23}$	7.9
16%	40.17	$1.55x10^{27}$	0.0034	$6.07x10^{24}$	3.9
Region(2)					
Content of SWCNT	T_0	$\eta(cm^{-3}/mev$	**$Rx10^{-7}$ (cm)**	**N (cm^{-3})**	**E (mev)**
4%	$8.6X10^{4}$	$7.24x10^{23}$	.231	$1.92x10^{22}$	26
8%	$2.59X10^{7}$	$2.4x10^{21}$	.096	$2.65x10^{20}$	110
12%	$7.75x10^{3}$	$8.04x10^{24}$	0.126	$1.19x10^{23}$	14.8
16%	$1.87X10^{3}$	$3.33x10^{25}$	0.0089	$8.19x10^{22}$	2.5
Region(3)					
Content of SWCNT	**T_0 (K)**	$\eta(cm^{-3}/mev$	**$Rx10^{-7}$ (cm)**	**N (cm^{-3})**	**E (eV)**
4%	$4.25x10^{5}$	$1.47x10^{23}$	0.345	$5.81x10^{21}$	0.039
8%	$3.17x10^{3}$	$1.96x10^{25}$	.1015	$2.28x10^{23}$	0.0116
12%	$2.51x10^{2}$	$2.47x10^{26}$	0.0054	$1.53x10^{24}$	.00620

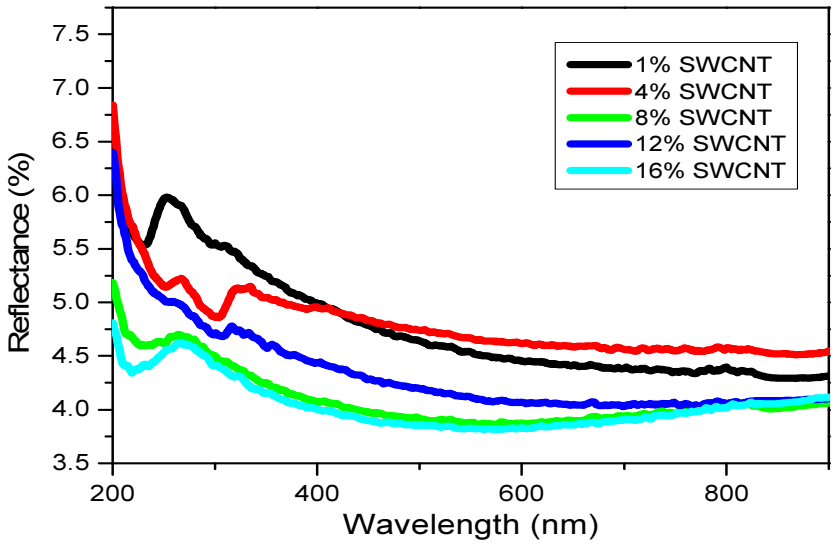

Fig. 1. Reflectance spectra of the PMMA –SWCNT nanocomposites

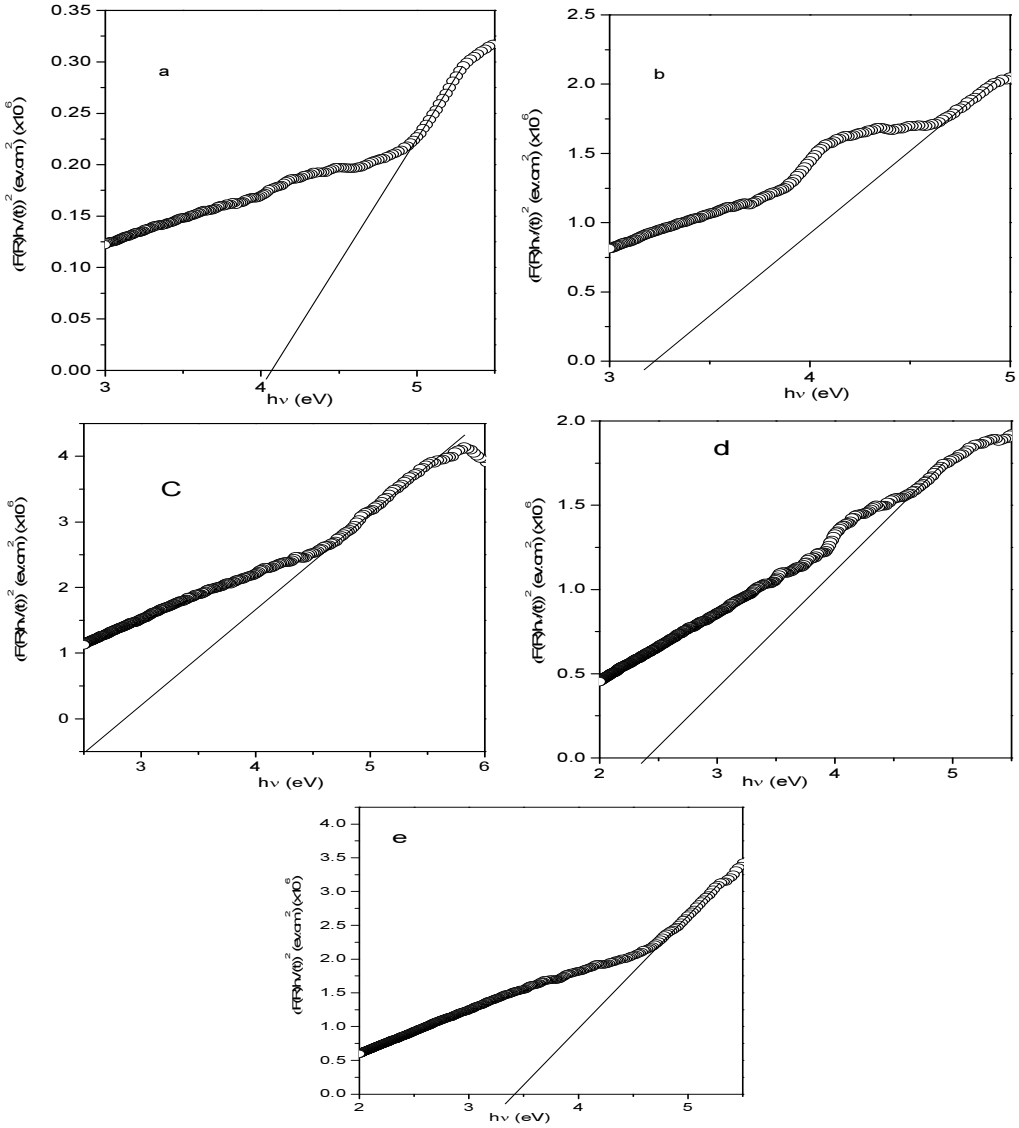

Figure 2: The plot of $(F(R)h\upsilon)^2$ versus the photon energy E for (a) PMMA-1%SWCNT, (b)PMMA-4% SW CNT,(c) PMMA-8%SWCNT, (d) PMMA-12%SWCNT. (e) PMMA-16%SWCNT

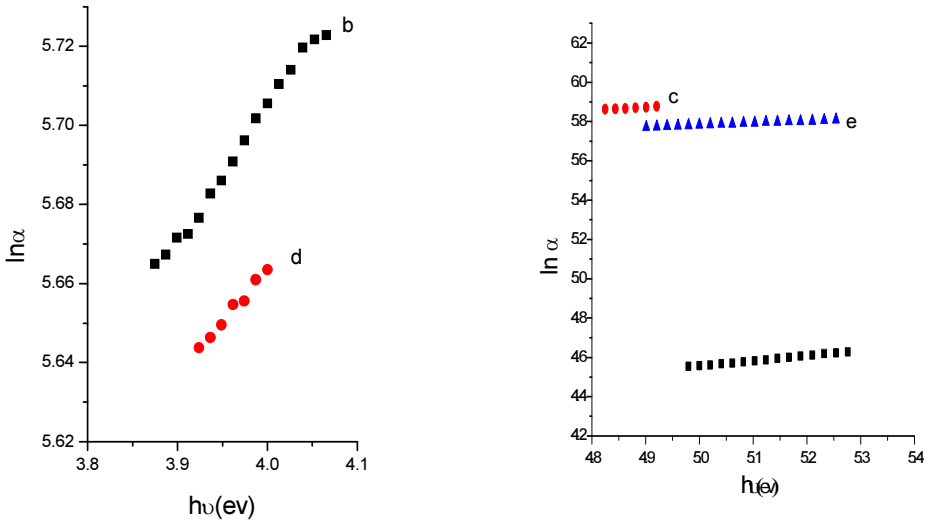

Figure(3) The dependence of ln(α) on photon energy E (ev) for (a) PMMA-1%SWCNT, (b)PMMA-4% SWCNT,(c) PMMA-8%SWCNT, (d) PMMA-12%SWCNT. (e) PMMA-16%SWCNT

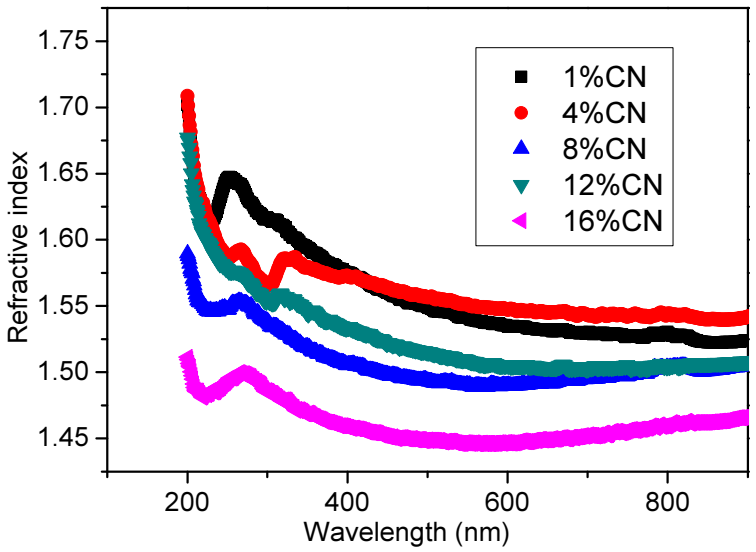

Figure (4) Variation of refractive index of PMMA –SWCNT composite with the applied wavelength.

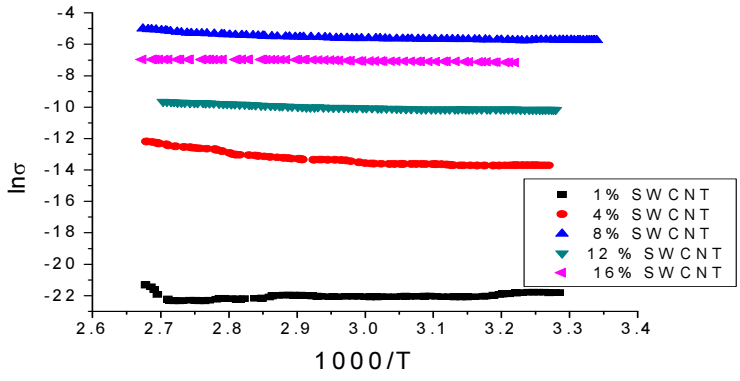

Fig.5 Plot of ln (σ) vs. 1000/T for PMMA-SWCNT composites

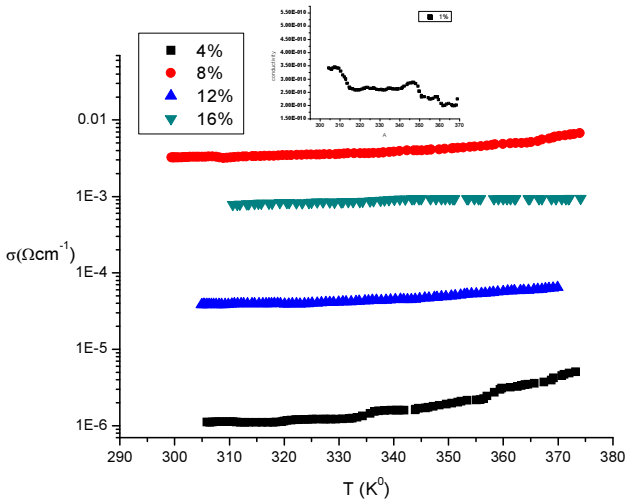

Fig.(6) Temperature dependence of electrical conductivity of PMMA-SWCNT composites

(a)

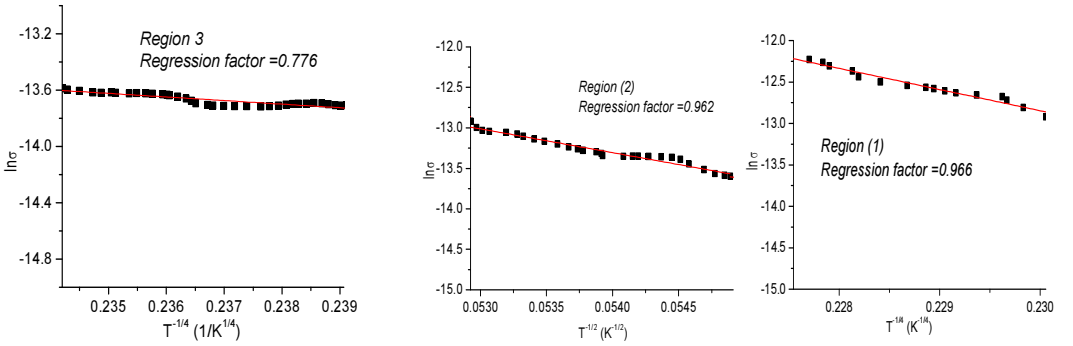

(b)

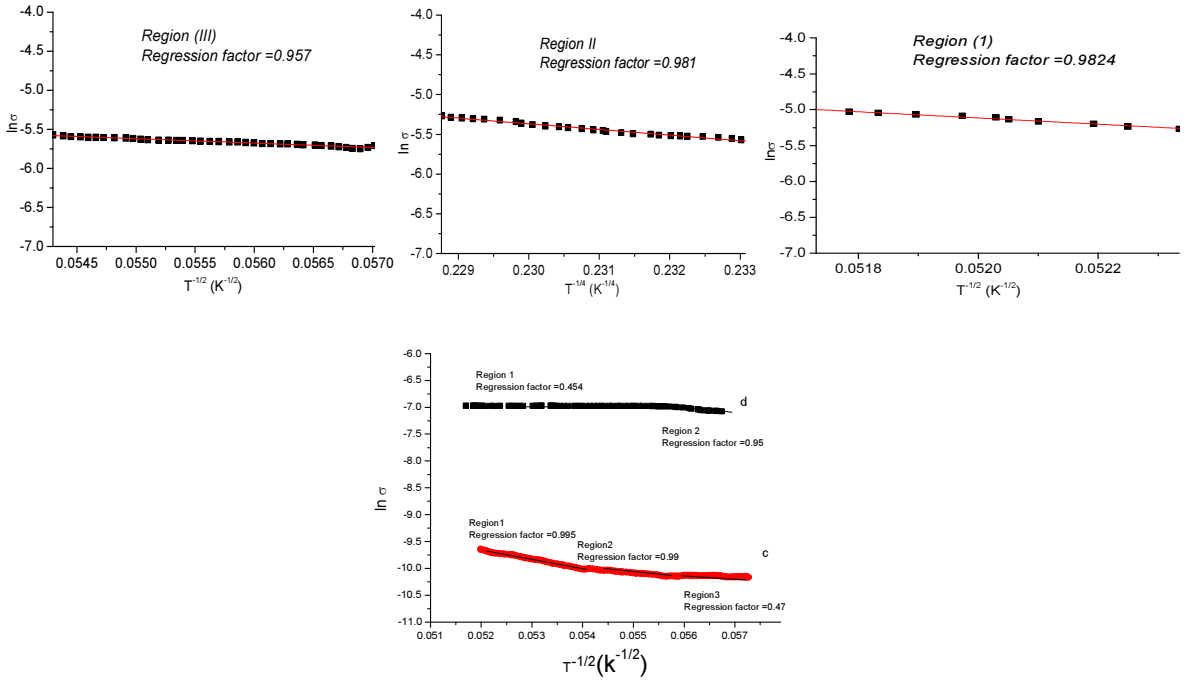

Fig.(7) Plots of lnσ vs. $T^{-1/4}$ and $T^{-1/2}$
(a) PMMA-4%SWCNT,(b) PMMA-%SWCNT (c) PMMA-12%SWCNT(d)PMMA-16%SWCNT

4. CONCLUSIONS

PMMA/SWCNT composites were prepared by coagulation method. The optical band energy of samples is decrease with SWCNT, the polymer matrix for all of the produced composites interact with dispersed SWCNT as demonstrated by the following points:

1- The energy gap E_g which indicates a transition of direct type and it decreases as the concentration of CNT increase up to 12%

2-. The shift of absorption edge is associated with a shrinkage effect

2- The electrical conductivity of PMMA matrix were not affected by the addition of low CNT concentration, meanwhile it increases as the filling ration increase and show the value close to that of semicrystalline mater .

Acknowledgement

This work was supported by Electronic Materials and Nanotechnology laboratory in Physics Department, Fırat University, Elazığ, TURKEY

REFERENCES

[1] A. Jamal, R. Ali, A. Somayeh, J. Macromol. Sci. Part B Phys. 35 (2007) 877.
[2] JN. Coleman, U. Khan, WJ. Blau, YK. Gun'ko. Small but strong: A review of the mechanical properties of carbon nanotube-polymer composites. Carbon 44 (2006) 1624-52
[3] Z. Spitalsky, D. Tasis, K. Papagelis, C. Galiotis. Prog Polym Sci 35 (2010) 357-401.
[4] M. Hameed Abdul-Allah, S. Salman Chiad, N. Fadhil Habubi, Diyala journal for pur science, 6 (2010).
[5] B. Zhang, F. D. Blum, Thermochim. Acta, 396, (2003). 211.
[6] H. Kaczmarek, H. Chaberska, Appl. Surf. Science, 252, (2006) 8185.
[7]. YL Huang., SM Yuen, Ma CCM, CY Chuang, Yu KC, CC Teng, HW Tien, YC Chiu, Wu SY, SH Liao, FB Weng.. Compos Sci Technol 69 (2009), 1991-6
[8] RH. Schmidt, IA. Kinloch, AN. Burgess, AH. Windle. The Effect of Aggregation on the Electrical Conductivity of Spin-Coated Polymer/Carbon Nanotube Composite Films. Langmuir (2007) 23, 5707–12.
[9] DO. Kim, MH. Lee, JH. Lee, TW. Lee, Kim KJ, YK. Lee,T. Kim, HR. Choi, JC. Koo, JD. Nam. Transparent flexible conductor of poly (methyl methacrylate) containing highly dispersed multiwalled carbon nanotube. Org Electron 9 (2008); 1-13.
[10] Y. Li, XC. Wang, MJ. Yang. n-Type gas sensing characteristics of chemically modified multi-walled carbon nanotubes and PMMA composite. Sens Actuators, B 121 (2007) 496-500.[
[11] S. Shang, L. Li, X. Yang, Y. Wei, Polymethylmethacrylate-carbon nanotubes composites prepared by microemulsion polymerization for gas sensor. Compos Sci Technol (2009), 69, 1156-9.
[12] D. Dorranian, Z. Abedinia, A. Hojabria, M. Ghoranneviss, Journal of Non-Oxide Glasses Vol. 1, No. 3, September (2009), 217 - 229
[13] P.Kubleka and F. Munk, Z.Phsysik, 12(1931) 593.
[14] The Kubelka-Munk theory of Reflectance,
www.ppfrs.org.uk/ianson/paper_physics/kubelka-Munk.html 30.6.2005 [20]
[15] E.Yassitepe,Z. Khalifa,G.H.Jaffari, C.S. Chou, S.Zulfiqar, M.I.Sarwar, S.I. Shah. p
[16] M. Jafari1, D. Dorranian2, Journal of Theoretical and Applied Physics, 5-2, (2011) 59-66
[17] F. Yakuphanoglu, G. Barim, I. Erol, Physica B 391, 136 (2007).
[18] S. Saravanan, M. R. Anantharaman, S. Venkatachalam, D. K. Avasthi; Vacuum (2007).
[19] H. M. Zidan, M. Abu-Elander, Physica. B 355, 308 (2005).
[20] R.M. Ahmed, International Journal of Photoenergy Volume 2009, Article ID 150389, 7 .
[21] M. F. Kotkata, H. T. El Shair, M. A. Afifi, andM.M. Abdel Aziz, Journal of Physics D, 27, 3, (1994). 623–627.
[22] F.Urbach Phys.Rev.92, (1953) 1324.
[23] PM .Ajayan, O. Stephan, C. Colliex, D. Trauth. Science 4 (1994) 265:1212-.
[24] E. Burstein, Phys. Rev. 93 (1954) 632. (b) T.S. Moss, Proc.Phys. Soc. london. B 67 (1954) 775.
[25] D. Dragoman, M. Dragoman, Optical characterization of solids, 1st edn. (Springer, Berlin, (2002)
[26] M. Caglar, S. Ilican, Y. Caglar, Thin Solid Films 517 (2009) 5023-5028
[27] S. Arrhenius, Z. Phys. Chem. 4, 226 _1889_
[28]- N. Mott, J. Non Cryst-Solids 1:1, (1968).
[29] I. G. Austin and N. F. Mott, Adv. Phys. (1969) 18:41
[30]- D. K. Paul, and S.S. Mitra , Phys. Rev. Lett. 31:1000 (1973).
[31] R. Gangopadhyay A. De and S. Das, J. Appl. Phys. 87:2363 (2000).
[32] R. Singh AK, RP. Tandon, A. Mansingh, S.Chandra, J. Appl Phys 79:1476 (1996).